Toxicology and Applied Pharmacology 375 (2019) 17–31

Contents lists available at ScienceDirect

Toxicology and Applied Pharmacology

journal homepage: www.elsevier.com/locate/taap

Pulmonary toxicity of two different multi-walled carbon nanotubes in rat: Comparison between intratracheal instillation and inhalation exposure

Laurent Gaté[a,*], Kristina Bram Knudsen[b], Carole Seidel[a], Trine Berthing[b], Laëtitia Chézeau[a], Nicklas Raun Jacobsen[b], Sarah Valentino[a], Håkan Wallin[c], Sébastien Bau[a], Henrik Wolff[d], Sylvie Sébillaud[a], Mylène Lorcin[a], Stéphane Grossmann[a], Stéphane Viton[a], Hervé Nunge[a], Christian Darne[a], Ulla Vogel[b,e], Frédéric Cosnier[a]

[a] Institut National de Recherche et de Sécurité, F-54519 Vandoeuvre-lès-Nancy Cedex, France
[b] National Research Centre for the Working Environment, DK-2100 Copenhagen, Denmark
[c] National Institute of Occupational Health, Oslo, Norway
[d] Finnish Institute of Occupational Health, FI-00251 Helsinki, Finland
[e] Department for Micro- and Nanotechnology, Technical University of Denmark, DK-2800, Kgs. Lyngby, Denmark

ARTICLE INFO

Keywords:
Carbon nanotubes
Inhalation
Intratracheal instillation
Rat
Lung inflammation

ABSTRACT

Multi-walled carbon nanotubes (MWCNTs), which vary in length, diameter, functionalization and specific surface area, are used in diverse industrial processes. Since these nanomaterials have a high aspect ratio and are biopersistant in the lung, there is a need for a rapid identification of their potential health hazard. We assessed in Sprague-Dawley rats the pulmonary toxicity of two pristine MWCNTs (the "long and thick" NM-401 and the "short and thin" NM-403) following either intratracheal instillation or 4-week inhalation in order to gain insights into the predictability and intercomparability of the two methods. The deposited doses following inhalation were lower than the instilled doses. Both types of carbon nanotube induced pulmonary neutrophil influx using both exposure methods. This influx correlated with deposited surface area across MWCNT types and means of exposure at two different time points, 1–3 days and 28–30 days post-exposure. Increased levels of DNA damage were observed across doses and time points for both exposure methods, but no dose-response relationship was observed. Intratracheal instillation of NM-401 induced fibrosis at the highest dose while lower lung deposited doses obtained by inhalation did not induce such lung pathology. No fibrosis was observed following NM-403 exposure.

When the deposited dose was taken into account, sub-acute inhalation and a single instillation of NM-401 and NM-403 produced very similar inflammation and DNA damage responses.

Our data suggest that the dose-dependent inflammatory responses observed after intratracheal instillation and inhalation of MWCNTs are similar and were predicted by the deposited surface area.

1. Introduction

Multi-walled carbon nanotubes (MWCNTs) exhibit physico-chemical properties, including electrical, mechanical and thermal properties that are promising for various applications. For example, MWCNTs are already used in numerous industrial products such as sporting goods and electronic parts. It was estimated that over 10,000 tons MWCNTs were produced in 2018 (Statistica, 2019). Since MWCNTs have high aspect ratios and are biopersistant in the lung, they share similarities with asbestos and may induce frustrated phagocytosis, inflammation, fibrosis and cancer (Porter et al., 2010; Donaldson and Oberdorster, 2011; Ravichandran et al., 2011; Wang et al., 2011; Donaldson et al., 2013; Porter et al., 2013; Kasai et al., 2015; Kasai et al., 2016; Suzui et al., 2016; IARC, 2017). MWCNTs vary in terms of length, diameter,

* Corresponding author at: Institut National de Recherche et de Sécurité, Département Toxicologie et Biométrologie, 1, rue du Morvan - CS 60027, F-54519 Vandoeuvre Cedex, France.
E-mail addresses: laurent.gate@inrs.fr (L. Gaté), carole.seidel@inrs.fr (C. Seidel), trb@nfa.dk (T. Berthing), nrj@nfa.dk (N.R. Jacobsen), sarah.valentino@inrs.fr (S. Valentino), hakan.wallin@stami.no (H. Wallin), sebastien.bau@inrs.fr (S. Bau), henrik.wolff@ttl.fi (H. Wolff), sylvie.sebillaud@inrs.fr (S. Sébillaud), mylene.lorcin@inrs.fr (M. Lorcin), stephane.grossmann@inrs.fr (S. Grossmann), stephane.viton@inrs.fr (S. Viton), herve.nunge@inrs.fr (H. Nunge), christian.darne@inrs.fr (C. Darne), ubv@nfa.dk (U. Vogel), frederic.cosnier@inrs.fr (F. Cosnier).

https://doi.org/10.1016/j.taap.2019.05.001
recibido en 2 marzo 2019; recibido en versión revisada en 30 abril 2019; aceptado en 4 mayo 2019
Available online 07 May 2019
0041-008X/ © 2019 Elsevier Inc. All rights reserved.

specific surface area, agglomeration state, functionalization, and metal-contaminant content, and this has been shown to affect their toxicological properties (Yamashita et al., 2010; Hamilton Jr. et al., 2013; Taylor et al., 2014; van Berlo et al., 2014; Poulsen et al., 2015; Poulsen et al., 2016; Poulsen et al., 2017; Knudsen et al., 2019). It is therefore important to be able to compare the toxicological profiles of many different MWCNTs in order to identify physical and chemical predictors of MWCNT toxicity for grouping, hazard ranking and the development of a safer-by-design approach. Inhalation is the most important route of exposure to CNTs, and their toxicity has been studied using oropharyngeal aspiration, intratracheal instillation or inhalation. The latter represents the most relevant approach for human exposure, but it is time consuming, expensive, and requires large quantities of material. In addition, the deposited dose depends strongly on the aerodynamic size, and is difficult to assess it empirically (Doudrick et al., 2013; Pauluhn and Rosenbruch, 2015; Ohnishi et al., 2016). On the other hand, aspiration or instillation are simple to do, allow for precise control of the deposited dose and the dose can be assumed to be independent of size distribution of the material. Some studies show that MWCNTs administered either by inhalation or intratracheal instillation induce pulmonary inflammation but the effects are more pronounced following intratracheal instillation since the MWCNT lung deposited dose is much higher (Morimoto et al., 2012; Silva et al., 2014). However, these studies do not directly compare the toxicity of similar lung deposited dose and only assess one type of MWCNTs (either pristine or surface-modified). It is then important to pursue the comparison of the pulmonary toxicity of MWCNTs following inhalation and instillation exposure and take into consideration their physical and chemical characteristics in order to bring additional data to highlight similarities and discrepancies.

In the current study, we aimed to analyze the pulmonary toxicological profiles of two very different pristine MWCNTs: NM-401 ("long and thick") and NM-403 ("short and thin"), the latter having a much larger BET specific surface area. Inhalation studies are expensive and complicated to perform. If intratracheal instillation testing is used to replace some inhalation studies it would result in great savings. We assessed the pulmonary toxicity following either sub-acute inhalation or intratracheal instillation in order to gain insights into the predictability and intercomparability of the two methods.

2. Material and methods

2.1. Carbon nanotubes

Pristine MWCNTs NM-401 and NM-403, were obtained from the Fraunhofer Institute for Toxicology and Experimental Medicine (Hannover, Germany) and the Joint Research Centre (Ispra, Italy) respectively. The CNT samples were fully characterized in earlier works (Rasmussen et al., 2014; Poulsen et al., 2017) and their main physical and chemical characteristics are presented in Table 1.

2.2. Inhalation experiments

Animal experiments were performed according to EC Directive 2010/63/UE, in compliance with French regulations related to the protection of animals used for scientific purposes. Experimental procedures were approved by the local Ethical Committee and registered by the French Ministry for Research and Higher Education (APAFIS # 3468). The INRS animal facility has also been approved by the French Ministry of Agriculture (Agreement # D54-547-10). Thirteen-week-old female Sprague Dawley rats were purchased from Janvier Labs (Le Genest Saint Isle, France). They were housed in individually ventilated cages (Tecniplast) maintained in 12 h/12 h light/dark cycles, and when not in restraining tubes had *ad libitum* access to food and water.

The general experimental procedure is illustrated in Fig. 1. In brief, following acclimatization to the restraining tubes, animals were nose-only exposed by inhalation, 2 × 3 h/day, 5 days/week for 4 weeks, to filtered air or to aerosols of MWCNTs. Animals were euthanized 3, 30, 90, and 180 days after the end of exposure in order to assess the short- and long-term biological effects of the nanomaterials (Fig. 1).

2.3. Intratracheal instillation experiments

Animal experiments were performed according to EC Directive 2010/63/UE, in compliance with Danish regulations related to the protection of animals used for scientific purposes. Experiments with animals were approved by The Danish Ministry of Justice, Animal Experiments Inspectorate (permission 2006/561-1123). Seven- to eight-week-old female Sprague Dawley rats (average weight 188.6 ± 8.2 g) were obtained from Taconic Europe (Ejby, Denmark). Rats were allocated arbitrarily to the experimental groups and were acclimatized for 1 week before the start of experiments. The rats were housed in polypropylene cages with bedding (sawdust) and enrichment under controlled environmental, as previously described (Kyjovska et al., 2015). Rats had *ad libitum* access to food (Altromin 1324) and tap water (Kyjovska et al., 2015).

Rats were instilled intratracheally following previously described procedures (Jackson et al., 2011; Jacobsen et al., 2015). In brief, rats were anesthetized using 4–5% isoflurane with a flow of 80% oxygen in the chamber until fully relaxed. A 400 µL suspension was instilled followed by 200 µL air with a 1 mL plastic syringe. After the procedure, each rat was weighed and, after full recovery in their home cage, transferred to the animal facility. Animals were then euthanized 1 or 28 days after exposure (Fig. 1).

2.4. Experimental setup for animal exposure to carbon nanotubes

Animal exposures to nanostructured MWCNT aerosols were performed in a nose-only inhalation facility. Two concentrations were tested (0.5 and 1.5 mg/m^3). Aerosols were generated with an acoustic generator (McKinney et al., 2009) and delivered simultaneously to animals maintained in nose-only restraining tubes placed in 9-port nose-only inhalation chambers (EMMS, UK). In parallel, control rats were exposed in a similar way to filtered air. The aerosol and filtered air were conditioned at a temperature of 22 ± 2 °C and a relative humidity of 55 ± 10% in order to respect the physiological needs of the animals. Aerosol monitoring and in-depth characterization were ensured by 1) the use of real-time devices: an Optical Particle Sizer (OPC FIDAS mobile, Palas); a Condensation Particle Counter (CPC) (TSI model 3007); a Scanning Mobility Particle Sizer (SMPS, Grimm) composed of a Vienna-type Differential Mobility Analyzer and a CPC; an aerodynamic particle sizer (TSI APS model 3321); and an Electrical Low Pressure Impactor (ELPI, Dekati), and 2) samples taken for off-line analysis (gravimetric analysis, mass size distribution from cascade

Table 1
Characteristics of the carbon nanotubes.

	Length (µm)	Diameter (nm)	S_{BET}* (m^2/g)	Purity (%)	Metal content (wt%)	Powder density (g/cm^3)
NM-401	4.0 (± 0.37)	67 (24–138)	18	98	Fe 0.05, Mg 0.015	0.02
NM-403	0.4 (± 0.03)	12 (5–37)	135	96.9	Fe 0.002, Mg 0.188, Co 1.2, Ni 0.0018, Mn 0.16	0.17

* S_{BET}: Specific surface area determined by Brunauer, Emmett and Teller method.

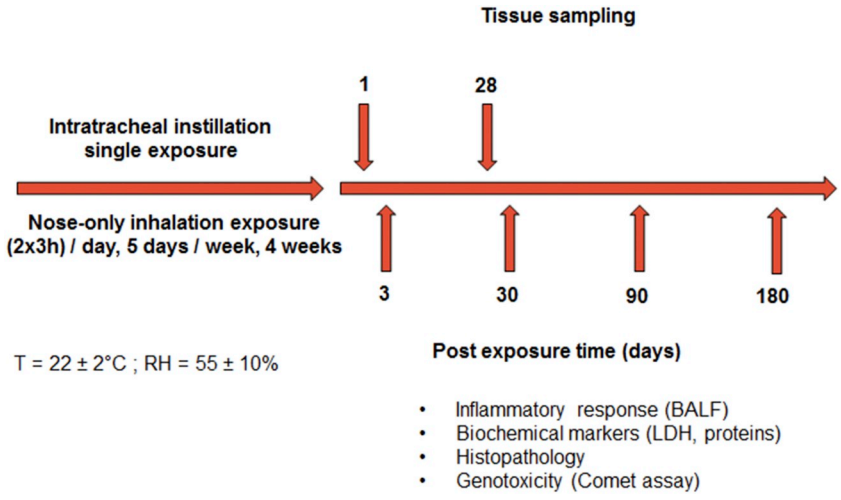

Fig. 1. Experimental protocol.
Rats were nose-only exposed for 2x3h/day, 5 days/week for 4 weeks and tissues were sampled at 3, 30, 90, and 180 days post-exposure or *via* single intratracheal instillation with sampling conducted 1 and 28 days post-exposure. Inflammatory response, biochemical markers, histopathology and genotoxicity were analyzed. BALF: Broncho-alveolar lavage fluid, LDH: Lactate dehydrogenase.

impactor (SIOUTAS, SKC), and TEM observations). The characterization strategy has been described previously (Cosnier et al., 2016).

Nanomaterial dispersions used for IT were prepared following a previously described procedure (Poulsen et al., 2015). The MWCNT stock dispersions were prepared in a concentration stock of 2.56 mg/mL in 0.45 µm MilliQ filtered Nanopure water with 2% rat serum. Dispersions were sonicated in a volume of 4–6 mL for 16 min using a 400 W Branson Sonifier S-450D (Branson Ultrasonics Corp., Danbury, CT, USA) mounted with a disruptor horn and operated at 10% amplitude. The dispersions were continuously cooled by ice/water. The dilution used for instillation was prepared directly after sonication and was further sonicated for 2 min after re-suspension.

2.5. Pulmonary deposition after inhalation

Pulmonary deposition after inhalation was estimated from the MPPD model (v.3.04) using the asymmetric Sprague-Dawley airway morphometry (Anjilvel and Asgharian, 1995; Miller et al., 2014) (https://www.ara.com/products/multiple-path-particle-dosimetry-model-mppd-v-304). In order to calculate the lung deposition of inhaled particles, several variables must be estimated. The physiological parameters used were the default values of MPPD determined for a given rat weight (which may differ slightly from one experiment to another) (Miller et al., 2016), for example, functional residual capacity (FRC) = 3.45 mL, upper respiratory tract volume (URT) = 0.41 mL, breathing frequency = 166 breaths/min, tidal volume = 2.08 mL and inspiratory fraction = 0.5, for a rat of 295 g.

Considered more robust than count median diameters for this purpose (Oberdorster et al., 2015), MMAD and their associated GSD (Table 2) were used in the calculations. GSD were determined from a log-normal fitting of the number size distribution provided either by SMPS or APS measurements; alternatively, they can be calculated according to Eq. (1).

$$GSD = exp\left[\sqrt{\frac{1}{3} ln\left(\frac{MMAD}{CMAD}\right)}\right] \quad (1)$$

In addition, the real mean aerodynamic effective densities ($\overline{\rho_e}$) of the aerosols, calculated from particle size distributions and gravimetric sampling data (Eq. (2)), were preferred to the bulk densities of the powders.

$$\overline{\rho_e} = \frac{C_M}{\sum_d \frac{\pi d^3}{6} C_N(d)} \quad (2)$$

Finally, although very important for estimating deposition fractions, values of aspect ratios are difficult to determine. The decision was made to consider the mean aspect ratios of the aerosols rather than those of the original CNTs. This seems particularly appropriate for NM-403 aerosols, which, like the Baytubes MWCNTs used by Pauluhn, are spherical to oval in shape (with an aspect ratio ≤ 8) and have a somewhat frayed surface and thus a mean aspect ratio of 4 (Pauluhn 2010a,b). It is less clear however for NM-401; the mean aspect ratio was assumed to be 30 because the NM-401 aerosols are composed of quite spherical agglomerates but also contain isolated CNTs (aspect ratio = 4/0.067 = 60). Any interpretations must be made in the light of the important uncertainties resulting from these choices.

2.6. Necropsy and tissue sampling

For tissue collection, animals exposed by inhalation were anesthetized by an intraperitoneal injection of pentobarbital (60 mg/kg). Rats were euthanized by exsanguination through the abdominal aorta.

On the necropsy day, rats exposed by IT were weighed and anesthetized by an intraperitoneal Injection with a ZRF cocktail (Zoletil Forte 250 mg/mL, Rompun 20 mg/mL, Fentanyl 50 µg/mL in sterile isotone saline, dose 1 mL/250 g bodyweight). Heart blood was withdrawn using a 21 G needle with a 5 mL syringe and stabilized with K_2EDTA.

Table 2
Main characteristics of the aerosols.
The actual mass concentration was derived from two daily gravimetric samplings for 0.5 mg/m^3 and four daily samplings for 1.5 mg/m^3.

	Target concentration (mg/m^3)	Actual mass concentration (mg/m^3)	Number concentration (particles/cm^3)	MMAD (nm)	CMAD (nm)	GSD	Aerosol effective density (g/cm^3)*
NM-401	1.5	1.49 ± 0.24	2455 ± 260	790	280	1.83	0.36
	0.5	0.54 ± 0.11	670 ± 120				
NM-403	1.5	1.48 ± 0.63	445 ± 75	1940	1440	1.48	0.10
	0.5	0.50 ± 0.14	110 ± 25				

* Calculated from particle size distributions and gravimetric sampling.

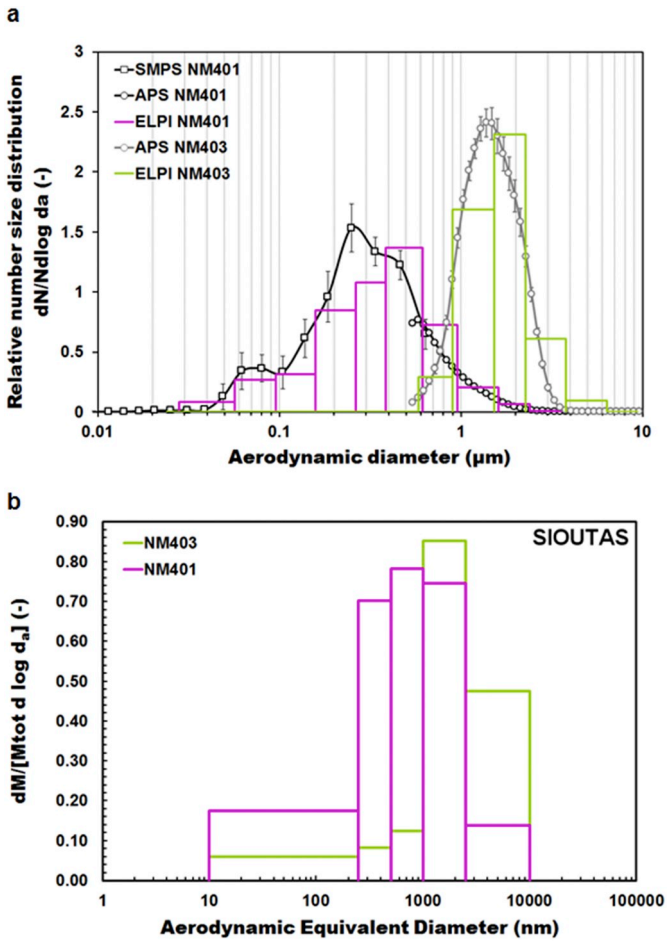

Fig. 2. Number (a) and mass (b) size distribution of the aerosols.

2.7. Tissue collection from inhalation exposed animals

BAL was performed on the left lung with 4 mL of ice-cold PBS. Four additional lavages were performed with 4 mL of ice-cold PBS each and collected in a separate tube. Both BAL were centrifuged 5 min at 4 °C at 400*g*. The supernatant from the first tube was used for biochemical analysis using a Randox analyzer. The supernatant from the second tube was discarded and the two cell pellets were resuspended in ice-cold PBS for cytology analysis and comet assay. BAL cytology analyses were performed on cytospin preparation stained with May-Grünwald-Giemsa technique, 500 cells/animal were then analyzed. The right caudal lung lobe was used for histopathology analysis.

For the comet assay, the left lung was dissociated by enzymatic technique using Collagenase type IA (Sigma Aldrich) and Miltenyi Biotec Gentle Max dissociator.

2.8. Tissue collection from intratracheal instillation exposed animals

Lungs were flushed twice with 5 mL sterile 0.9% NaCl through the trachea to obtain the BAL. Only BAL fluid from the first flush was used for further biochemical analysis. BAL cells from both flushes were used for further cell analysis. Lung tissue was collected, sectioned, snap frozen in liquid nitrogen, and then stored at −80 °C. The BAL was stored on ice until centrifugation at 800*g* for 6 min at 4 °C to separate BAL fluid from BAL cells. The acellular BAL fluid from the first flush was stored at −80 °C. The BAL cells from both flushes were re-suspended in 1 mL medium (HAM F-12 with 1% penicillin/streptomycin and 10% fetal bovine serum). The total number of living and dead cells in the BAL was determined by NucleoCounter NC-200TM (Chemometec, Denmark). Samples for the comet assay were prepared from 40 µL re-suspended BAL cells and 60 µL of ice-cold media (HAM F-12, 1% penicillin/streptomycin, 15% fetal bovine serum and 10% DMSO). Samples were divided into three aliquots and immediately frozen at −80 °C. An additional sample of the cell re-suspension was used to estimate the number of granulocytes (neutrophils and eosinophils), macrophages, lymphocytes and epithelial cells in the BAL fluid. The cell suspension was centrifuged in a Cytofuge 2 (StatSpin, TRIOLAB, Brøndby, Denmark) and fixed for 5 min in 96% ethanol. All slides were stained with May-Grünwald-Giemsa stain, randomized and blinded before counting 200 cells/sample.

2.9. Enhanced darkfield microscopy

The Cytoviva enhanced darkfield hyperspectral system (Auburn, AL, USA) was used to detect MWCNT in lung tissue, by manually scanning histological sections at 40 x in enhanced darkfield mode. The right caudal lung lobes were analyzed 3, 30, 90 and 180 days after inhalation and the left lung lobes were analyzed 28 days after instillation. Darkfield images were acquired at 100 x on an Olympus BX 43 microscope with a Qimaging Retiga 4000R camera.

2.10. Histopathology: inhalation experiments

Lung right caudal lobes were filled slowly with 4% neutral buffered formaldehyde under 30 cm water column pressure. A knot was made around the bronchia to secure formaldehyde in lungs to fixate tissue in 'inflated state'. Paraffin embedded tissue blocks of lung from animals exposed by inhalation to the highest concentrations of CNTs and their matched controls were analyzed for histopathology. Two staining protocols were used: the Hematoxylin-Eosin procedure for general histopathology and the Trichrome-Masson method for the deposition of collagen (a marker of fibrosis).

2.11. Histopathology: intratracheal instillation experiments

Lungs were filled slowly with 4% formalin under 30 cm water column pressure. A knot was made around trachea to secure formaldehyde in lungs to fixate tissue in 'inflated state'. The collected lungs from all groups were fixed in 4% neutral buffered formaldehyde solution for 24 h. After fixation, the organs were trimmed, dehydrated on a Leica ASP300S (Leica Systems) and embedded in paraffin. Sections were cut at 3 µm on a Microm HM 355S Microtome (Thermo Scientific™). Sections for light microscopic examinations were stained with Hematoxylin and Eosin (H&*E*- staining) or Sirius Red staining.

2.12. Comet assay: DNA damage analysis in samples from rats exposed by inhalation

The *in vivo* comet assay was performed as previously described (Guichard et al., 2015). Cells were mixed with 1% low-gelling agarose and poured onto microscope glass slides pre-coated with 1% routine agarose. The microscope slides were then laid on an ice bed to allow the agarose to solidify. Once the agarose had solidified, the slides were immersed in the ice-cold lysis buffer (2.5 mM NaCl; 100 mM Na_2EDTA; 10 mM Tris base; 10% DMSO and 1% Triton; pH 10) overnight at 4 °C. The next day, the slides were immersed in the ice-cold alkaline electrophoresis buffer (300 mM NaOH; 1 mM Na_2EDTA; pH > 13) for 20 min and then submitted to electrophoresis for 40 min at 0.9 V/cm. At the end of the electrophoresis, slides were immersed in the neutralization buffer (Tris base 0.4 M; pH 7.5) for 15 min at 4 °C. Slides were then washed once with ultrapure water for 5 min and dehydrated for 10 min into 96% ethanol before being dried at 45 °C and stored in the dark at room temperature. For fluorescent microscopy analysis, slides were rehydrated for 10 min with ultrapure water and then stained with propidium iodide 2.5 µg/mL in PBS. For each sample, 100 cells

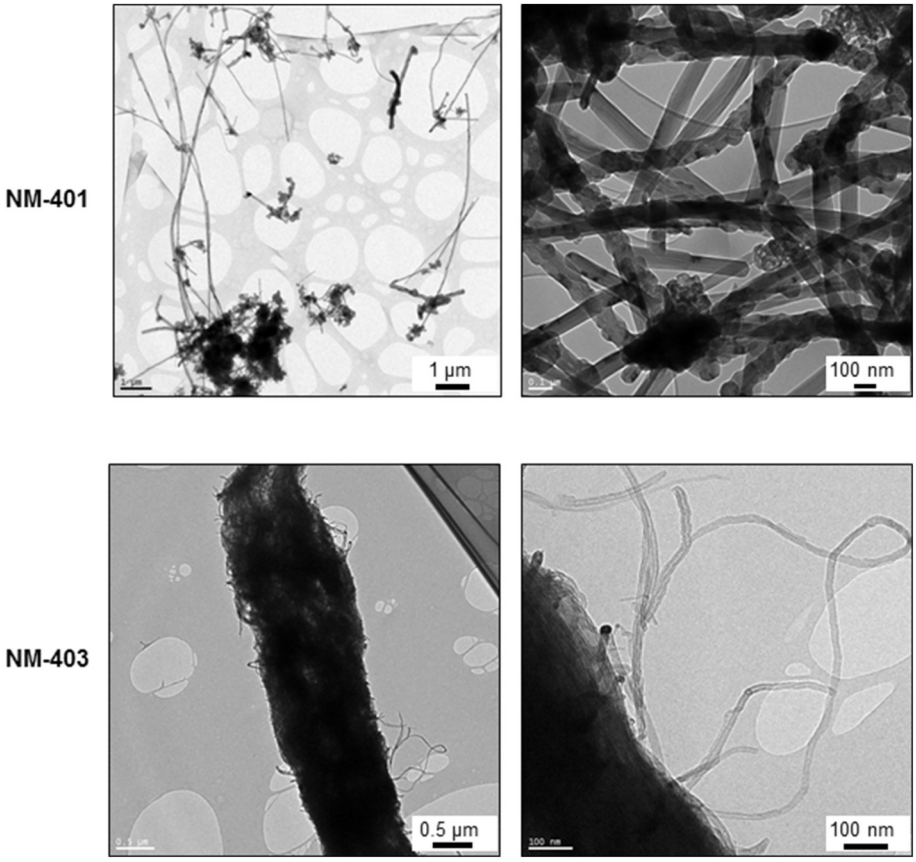

Fig. 3. Representative transmission electron microscopy images of NM-401 and NM-403 aerosols.
Carbon nanotubes aerosols were collected on TEM grids and observed with a Philips Transmission electron microscope equipped with a Gatan digital camera.

Table 3
MPPD model-estimated MWCNTdeposition in the respiratory tract for inhaled NM-401 and NM-403.

	Concentration (mg/m^3)	Mean rat weight (g)	Head fraction	TB fraction	P fraction	TB deposited amount (µg)*	P deposited amount (µg)*	Thoracic deposited amount (µg)*
NM-401	1.5	295	0.304	0.119	0.060	470	239	709
	0.5	415	0.318	0.095	0.045	189	90	279
NM-403	1.5	295	0.367	0.015	0.009	54	34	88
	0.5	295	0.327	0.008	0.004	15	7	22

TB: Tracheobronchial, P: Pulmonary, Thoracic = TB + P.
* Estimated deposited dose after the end of exposure (6 h/day, 5 days/week for 4 weeks).

were analyzed using the Comet Assay IV software (Perceptive Instruments, Suffolk, UK) and the percentage of DNA in the tail of each comet was measured.

The positive controls for comet assay were BAL and lungs cells from rats exposed by gavage to methyl methanesulfonate (MMS, Sigma Aldrich) to a final concentration of 25 mg/kg b.w. and 12.5 mg/kg b.w. 24 and 3 h before tissue collection respectively.

2.13. Comet assay: DNA damage analysis in samples from rats exposed by intratracheal instillation

DNA strand break levels were analyzed by the comet assay as described by (Jackson et al., 2013). The measured DNA strand breaks present a mixture of different strand breaks, alkaline labile sites and transient breaks in the DNA due to repair processes. DNA strand breaks were determined on BAL cell suspensions, lung (half of the left lobe). The sample preparation and analysis procedures have previously been described in detail (Jackson et al., 2013). In brief, BAL cells preserved in freezing media were thawed quickly at 37 °C, while frozen lung tissue was homogenized in Merchant's medium. Cells were suspended in agarose at 37 °C (final agarose concentration 0.7%), and then embedded on Trevigen CometSlides™ (30 µL per well for a 20 well slide). Cooled slides were placed in lysis buffer overnight at 4 °C. The next day, slides were rinsed in electrophoresis buffer and then alkaline treated for 40 min. Electrophoresis was run with 5% circulation (70 mL/min) for 25 min at an applied voltage of 1.15 V/cm (38 V) and a measured current of 300 mA. Slides were neutralized (2 × 5 min), fixed in 96% ethanol for 5 min and then placed on a 45 °C plate for 15 min. Cells were stained in a 20 mL/slide bath with TE buffered SYBR®Green fluorescent stain for 15 min and then dried at 37 °C for 10 min. A UV-filter and cover slip were applied and DNA damage was analyzed using the IMSTAR Pathfinder™ system. Related samples were placed in the same electrophoresis. The results are presented as the average %TDNA value for all cells scored in each Trevigen CometSlide well. The day-to-day variation and electrophoresis efficiency was validated by including wells of A549 epithelial lung cells exposed to either PBS or 60 µM H_2O_2 on each slide. These were used as negative and positive historical controls for the electrophoresis (Jackson et al., 2013).

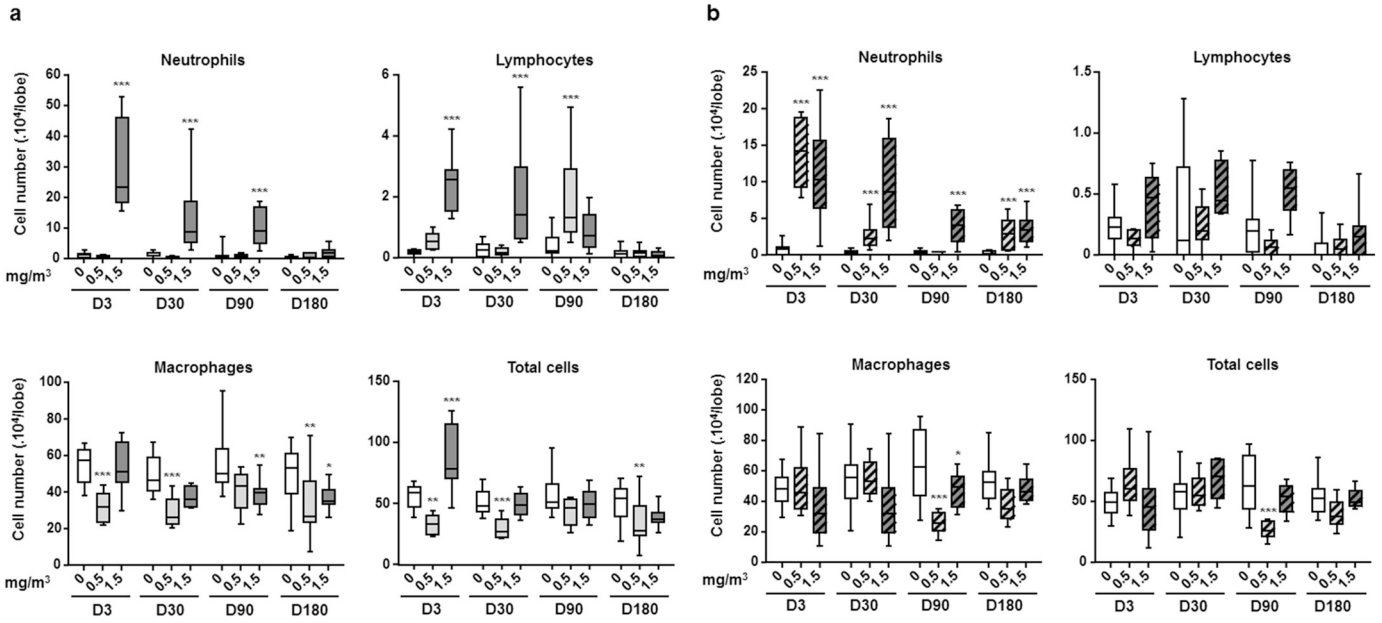

Fig. 4. Cytology of broncho-alveolar lavage fluid from the control and animals exposed to NM-401 or NM-403 by inhalation.
Broncho-alveolar lavage (BAL) fluid cell content was assessed by counting macrophages, neutrophil granulocytes and lymphocytes in BAL fluid collected 3, 30, 90 and 180 days after inhalation exposure to filtered air (control animals) or to 0.5 or 1.5 mg/m^3 of NM-401 (a) or NM-403 (b). * $p < .05$, ** $p < .01$, *** $p < .005$ Significantly different from the control.

2.14. Statistical analyses

Data are expressed as the median [Q1; Q3], with the first (Q1) and third quartiles (Q3) corresponding to 25 and 75% of scores, respectively. This graphical representation takes into consideration inter-individual variability and helps identifying extreme values and understanding the distribution of observations. A logarithmic transformation was applied to the data. For inhalation data, a mixed linear regression model was used to test the “dose” and “time” fixed effects, including a random effect “experiment” to take into account the experiment variability (since animal exposure to each dose of MWCNT aerosol was performed as an independent experiment) (nlme package, R, Pinheiro, Bates, DebRoy, Sarkar and the R Development Core Team 2013. nlme. R package version 3.4.3; www.r-project.org/). For IT data, a linear model was used, adjusted for time and dose.

3. Results

3.1. Inhalation exposure

3.1.1. Aerosol characterization

For both MWCNTs, animals were exposed to two aerosol concentrations: 0.5 and 1.5 mg/m^3. The average aerosol mass concentrations measured over one-month exposure were 0.54 ± 0.11 mg/m^3 and 1.49 ± 0.24 mg/m^3 for NM-401 and 0.50 ± 0.14 mg/m^3 and 1.48 ± 0.63 mg/m^3 for NM-403. Thus, they were close to the target concentrations. For the same mass concentration, the total number concentration of airborne particles of NM-401 was 5 to 6 times higher than the one of NM-403 (Table 1).

This difference is related to the particle size distributions of the aerosols (Fig. 2). Despite the fact that NM-403 is “short and thin”, the particles resulting from its aerosolization are much bigger in diameter than those resulting from aerosolization of the “long and thick” NM-401: the mass median aerodynamic diameter (MMAD) and count median aerodynamic diameter (CMAD) are approximately 1.9 and 1.4 µm respectively for NM-403 but approximately 0.3 and 0.8 µm for NM-401. It is worth noting that the size distribution of NM-401 is broader than the one of NM-403. The equivalent geometric standard deviations (GSD) were 1.48 and 1.83 for NM-403 and NM-401, respectively.

From transmission electron microscopy (TEM) analysis (Fig. 3), the difference in size appeared to be linked to extent of entanglement of the carbon nanotubes: while NM-401 nanotubes appeared as individual fibers of different lengths that were sometimes entangled, NM-403 CNTs were highly entangled and were organized into large structures that had not been torn apart during aerosolization as the acoustic generator is soft generator. At higher magnifications, thin nanotubes could be seen protruding from the entanglement (Fig. 3).

The mean aerodynamic effective densities of the aerosols, as calculated from particle size distributions and gravimetric sampling data, were 0.36 g/cm^3 for NM-401 and 0.10 g/cm^3 for NM-403. These values are consistent with those of Wang et al. (Wang et al., 2015) based on the outer tube diameter and with the observation that effective density decreased with increasing agglomerate size. For NM-401, this mean aerosol effective density is far higher than the bulk density of the powder (= 0.02).

3.1.2. Deposited doses

We estimated that 709 and 279 µg of NM-401 were deposited within the rats' thoracic region (tracheobronchial and pulmonary areas) after one month of inhalation at 1.5 and 0.5 mg/m^3, respectively. For NM-403, the amounts deposited were estimated to be much lower: 88 and 22 µg at 1.5 and 0.5 mg/m^3, respectively (Table 2). The large discrepancy between lung-deposited CNT fractions (amounts) is mainly due to size distribution and aspect ratio of the aerosols. In both cases, only one third of the deposited mass reached the pulmonary region, whereas two thirds were deposited in the tracheobronchial region.

3.2. Instillation exposure

The nanomaterial dispersions used for instillation were characterized by dynamic light scattering. The hydrodynamic diameters (z-average) of NM-401 and NM-403 agglomerates in the suspensions ranged from 560 to 710 nm and from 230 to 160 nm, respectively. The polydispersity indexes (an estimate of the width of the distribution) were 0.3–0.4 and 0.5–0.6, respectively, indicating rather narrow

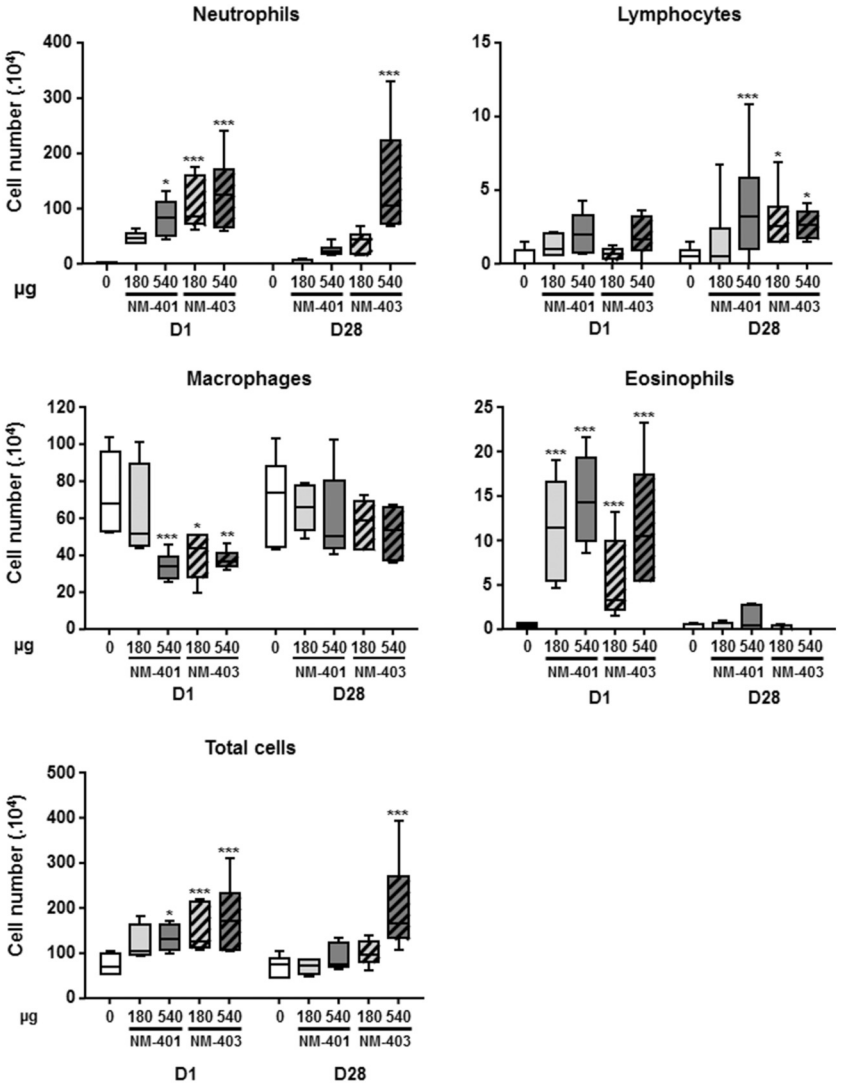

Fig. 5. Cytology of broncho-alveolar lavage fluid from the control and animals exposed to NM-401 or NM-403 by intratracheal instillation.
Broncho-alveolar lavage (BAL) fluid cell content was assessed by counting macrophages, lymphocytes, neutrophil and eosinophil granulocytes in BAL fluid collected 1 and 28 days after intratracheal instillation of 180 or 540 µg of NM-401 or NM-403. * $p < .05$, ** $p < .01$, *** $p < .005$ Significantly different from the control.

distributions. Contrary to what was observed in the aerosol phase and due to the use of serum and sonication, the NM-403 agglomerates were smaller than the NM-401 agglomerates (Table 3).

3.3. Bronchoalveolar lavage fluid cytology

Changes in bronchoalveolar lavage (BAL) fluid cell number and composition may be associated with toxicological processes and inflammatory response (especially a neutrophilic granulocyte influx). Sub-acute inhalation of the highest concentration of NM-401 (1.5 mg/m^3) led to a massive influx of neutrophilic granulocytes 3 days post-exposure ($p < .0001$). This influx diminished from a 20-fold increase at day 3 to a 10-fold increase at days 30 ($p < .0001$) and 90 ($p = .0002$) and was still visible, even though not significant, at 180 days post-exposure (Fig. 4a). An increase in lymphocyte numbers was also observed 3 days post-exposure ($p < .0001$) and declined over time. Surprisingly, sub-acute exposure to the lowest concentration of NM-401 (0.5 mg/m^3) led to a small but significant decrease in macrophages in the BAL fluid 3 ($p = .001$) and 30 days post-exposure ($p = .0002$). No change in neutrophilic granulocyte or lymphocyte abundance was observed for the lowest concentration, except at day 90 ($p < .0001$, Fig. 4a). The exposure to NM-403 led to a significant increase in the number of neutrophils (between 15 and 20-fold) for both concentrations 3 days after the end of exposure compared to matched air-exposed controls ($p < .0001$ for both doses, Fig. 4b). This influx was still observed after 30 ($p < .0001$ for both doses) and 90 days ($p < .0001$ for the highest dose), but it decreased in a dose-dependent manner. In addition, 180 days after the end of exposure, an increase in neutrophilic granulocytes was still significant for both doses of NM-403 ($p < .0001$). Lymphocyte cell number was not affected by exposure to NM-403 at any of the time points examined. Surprisingly, a decrease in macrophage numbers was observed 90 days post exposure in animals exposed to both doses of NM-403 ($p < .0001$ for the lowest dose, $p = .0305$ for the highest dose) (Fig. 4b).

In rats exposed by IT, exposure to both types of MWCNT increased the number of neutrophilic granulocytes, mostly after 1 day for the highest dose of NM-401 ($p = .0140$) and for both concentrations of NM-403 ($p = .0011$ for the lowest dose, $p = .0001$ for the highest dose, Fig. 5). After 28 days, only exposure to the highest concentration of NM-403 induced a neutrophilic granulocyte influx in BAL ($p < .0001$). Additionally, while the highest concentration of NM-401 ($p = .0029$) and both concentrations of NM-403 ($p = .0202$ for the lowest dose, $p = .0214$ for the highest dose) increased lymphocyte numbers after 28 days only, it decreased the number of macrophages only at day 1

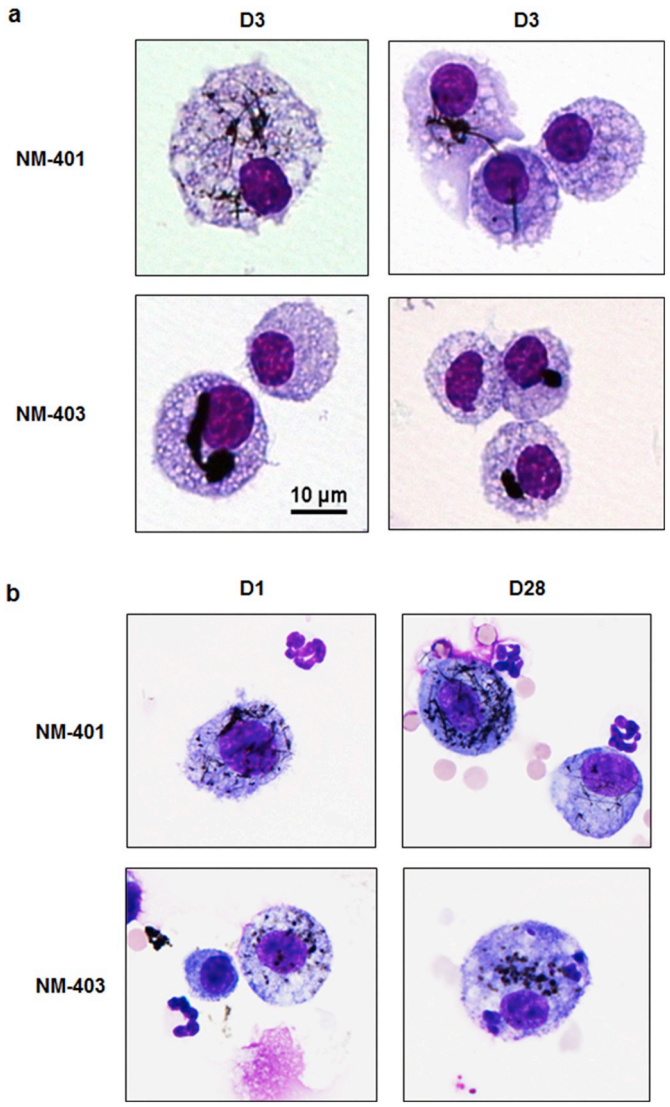

Fig. 6. Representative photomicrographs of MWCNT in BAL fluid macrophages. BAL fluid cells were cytospun on glass slides and stained with the May-Grünwald-Giemsa method from samples collected 3 days after sub-acute inhalation (a) or 1 and 28 days after intratracheal instillation (b). Scale bar 10 µm.

(p = .0022 for NM-401; p = .0219 for the lowest dose and p = .0068 for the highest dose of NM-403). Both MWCNTs at both concentrations significantly increased the number of eosinophils (p < .0001) but not in animals exposed by inhalation (Fig. 5).

The shapes of the nanomaterials found within BAL fluid macrophages from animals exposed by inhalation to NM-401 or NM-403 were similar to those observed on TEM grids (Fig. 6a). NM-401 MWCNTs in macrophages exposed by IT (Fig. 6b) looked similar in length and diameter to those observed after inhalation exposure, whereas NM-403 particles were much smaller after IT than after inhalation, in accordance with DLS measurements.

The neutrophil influx measured in the BAL fluid 1 day (for IT) or 3 days (for inhalation) after exposure to NM-401 and NM-403 correlated well with the deposited surface area in the lung (instilled or estimated just after the end of exposure) following a logarithmic curve (R^2 = 0.66) (Fig. 7a). This correlation was even stronger for longer post-exposure periods (R^2 = 0.80 at day 28 for IT and at day 30 for inhalation) (Fig. 7b).

3.4. Histopathology

Histopathological analyses following intratracheal instillation were performed on lung tissues from animals exposed to the highest concentration (*i.e.* 540 µg) of MWCNTs. In NM-401-exposed rats, macrophages containing black particles consistent with carbon nanotubes were observed (Fig. 8a), but the main finding was interstitial thickening accompanied by fibrosis (Fig. 8b). According to Wagner scale, we observed a histological grade 4 with minimal collagen deposition at the level of terminal bronchioles and alveoli (Fig. 8b). However, no increased bronchiolization was observed. In NM-403-exposed animals, the main findings were macrophages containing black particles, prominent macrophage activity and proteinaceous material in the alveoli in 4/6 rats, The proteinaceous material in alveoli observed was compatible with that seen in pulmonary alveolar proteinosis (PAP), it was not seen with the other exposures. Minor interstitial thickening was also observed but it was much less noticeable than in NM-401-exposed animals (Fig. 8a).

Histopathological analyses following inhalation exposure were also performed on lung tissues from animals exposed to the highest concentration (*i.e.* 1.5 mg/m^3) of MWCNTs (Fig. 8a). The most significant lung changes in NM-401 treated rats consisted in the presence of macrophages containing black particles consistent with carbon nanotubes between 3 and 180 days post-exposure. While the numbers of CNT-positive macrophages observed in exposed animals at 3, 30 and 90 days post-exposure were similar, their distribution in the lung sections differed (Fig. 8a). Singular, positive macrophages in the 3-day group were randomly disseminated throughout the lung section, mainly in alveoli. In the 30-day post-exposure group, positive macrophages were present not only in alveoli, but also as discrete aggregates associated with terminal bronchioles. In the 90-day post-exposure group, fewer positive cells were observed in alveoli and more prominent numbers of aggregates were associated with bronchioles. At 180 days post-exposure, a smaller number of positive macrophages were present in alveoli, and the number of macrophage aggregates associated with bronchioles was reduced.

No significant difference in the amount or distribution of collagen in the lung was observed with the Masson's Trichrome stain in control and exposed animals (data not shown).

At sacrifices on days 3, 30, 90 and 180, all NM-403-exposed rats showed accumulation of dark material in the cytoplasm of alveolar macrophages in the lungs. This was considered to likely reflect accumulation of NM-403 in alveolar macrophages and it was not accompanied by any treatment-related inflammatory change or other alteration of the lung parenchyma (Fig. 8a). No exposure-related changes (such as interstitial fibrosis) were observed in the Masson's trichrome stained sections of lung obtained from control and treated rats sacrificed on days 90 and 180 post-exposure (data not shown).

3.5. Pulmonary distribution of NM-401

The pulmonary distribution of NM-401 was analyzed using enhanced darkfield microscopy, which allows detection of single MWCNTs in histological samples (Fig. 9). The enhanced darkfield microscopy revealed that in addition to mainly being phagocytized by alveolar macrophages, single or small bundles of NM-401 were also present in the interstitium after both types of exposure and at all time-points analyzed (3, 30, 90 and 180 days post-inhalation and 28 days post-instillation). Twenty-eight days after instillation, bundles of NM-401 were observed close to some pulmonary blood vessels, as shown in Fig. 9. This was not observed after exposure *via* inhalation.

3.6. Bronchoalveolar lavage fluid biochemistry

In BAL fluid, increases in lactate dehydrogenase (LDH) activity and protein content are often signs of pulmonary toxicity following

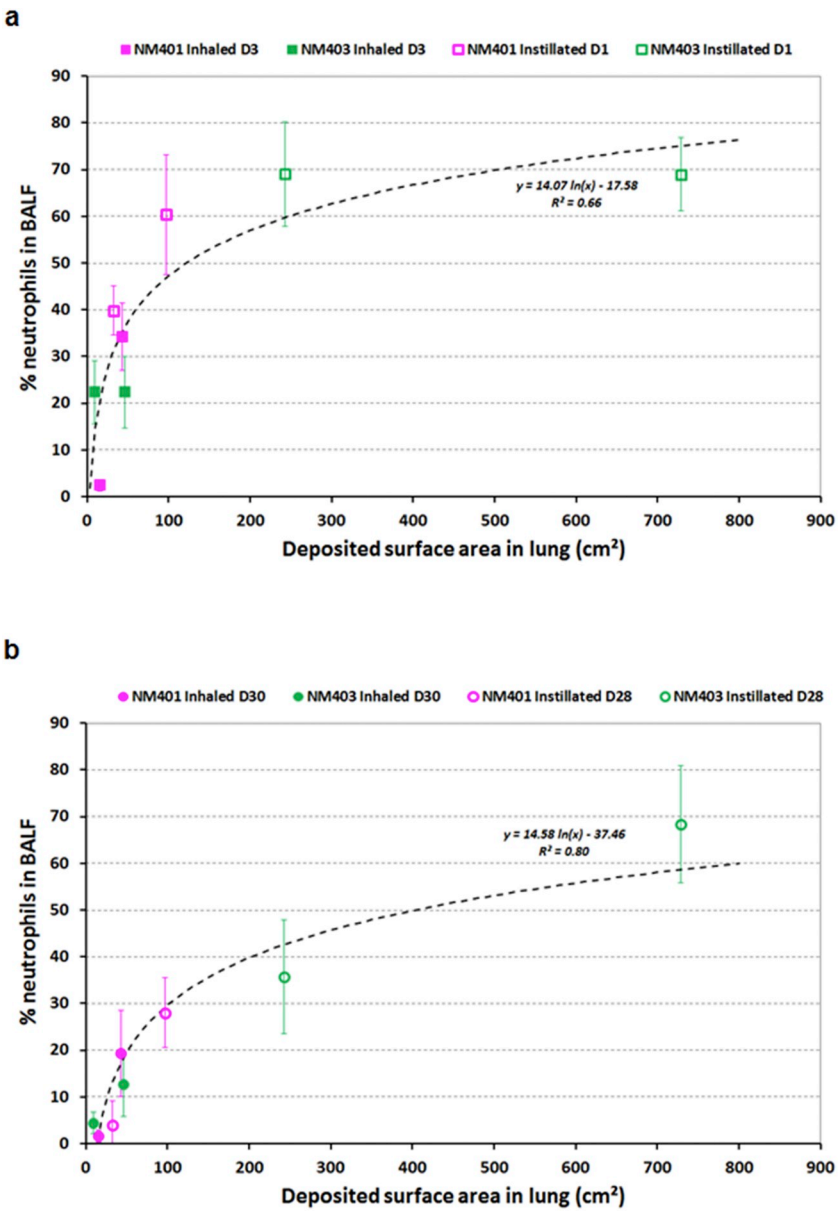

Fig. 7. Correlation between the percentage of BALF neutrophils and the pulmonary MWCNT-deposited surface area. (a) Percent neutrophils in BAL fluid on day 1 (IT) or 3 (inhalation) as function of pulmonary deposited surface area (estimated in the lung at the end of exposure) of rats exposed to NM-401 and NM-403 by inhalation (full square) or IT (open square). (b) Percentage of neutrophils in BAL fluid on day 28 (IT) or 30 (inhalation) as a function of pulmonary deposited surface area (estimated in the lung at the end of exposure) of rats exposed to NM-401 and NM-403 by inhalation (full square) or IT (open square). The logarithmic curves "models" were established from the set of individual data.

exposure to particulate matter. LDH activity and protein contents in BAL fluid were significantly higher 3 days after the end of exposure for both concentrations of NM-401 (LDH activity: $p = .0129$ and $p < .0001$ for the lowest and highest doses respectively; protein content: $p = .007$ and $p < .0001$ for the lowest and highest doses respectively) and NM-403 ($p < .0001$ for both doses and both parameters, Fig. 10) used. No or little significant change in protein content or enzyme activity was observed 30 and 180 days after exposure to NM-401 (Fig. 10a). Some significant changes in LDH activity as well as protein contents were however observed at 90 days post-exposure (LDH activity: $p = .003$ and $p < .0001$ for the lowest and highest doses respectively; protein content: $p = .0003$, $p = .0006$ for the lowest and highest doses respectively). Slight changes in BAL fluid biochemistry were observed 30, 90 and 180 days after the end of exposure to NM-403 (Fig. 10b).

3.7. DNA damage

The comet assay was performed to assess DNA strand breaks in lung and BAL cells induced following rat exposure to NM-401 or NM-403 by inhalation or IT (Fig. 11). Exposure to the lowest dose of NM-401 induced DNA damage in lung tissue only at day 30 in rats exposed by inhalation ($p = .005$, Fig. 11a). No genotoxicity was observed in the lung in rats exposed to NM-401 by IT (Fig. 11c). In the BAL cells, the lowest concentration of NM-401 administrated by IT induced DNA damage at day 28 ($p = .0096$, Fig. 11c). Inhalation of the lowest concentration of NM-403 decreased DNA strand breaks in lung ($p = .0126$) and BAL cells ($p = .0017$) at day 3, however DNA strand break levels were increased at day 30 ($p = .0001$ in lung tissue, $p = .271$ in BAL cells, Fig. 11b). A slight but significant decrease in DNA damage levels was observed only at day 180 in BAL cells ($p = .0002$). The highest concentration of NM-403 increased DNA damage in the lung tissue at day 90 ($p = .0001$) after exposure by inhalation and at day 1 ($p = .0109$) after IT exposure (Fig. 11b and c). Thus, increased levels of DNA strand breaks were observed across doses and time points for both exposure methods. However, no consistent dose-dependent responses were observed for either exposure method.

4. Discussion

MWCNTs are used in many industrial processes, and occupational exposure by inhalation is a primary concern for workers' health.

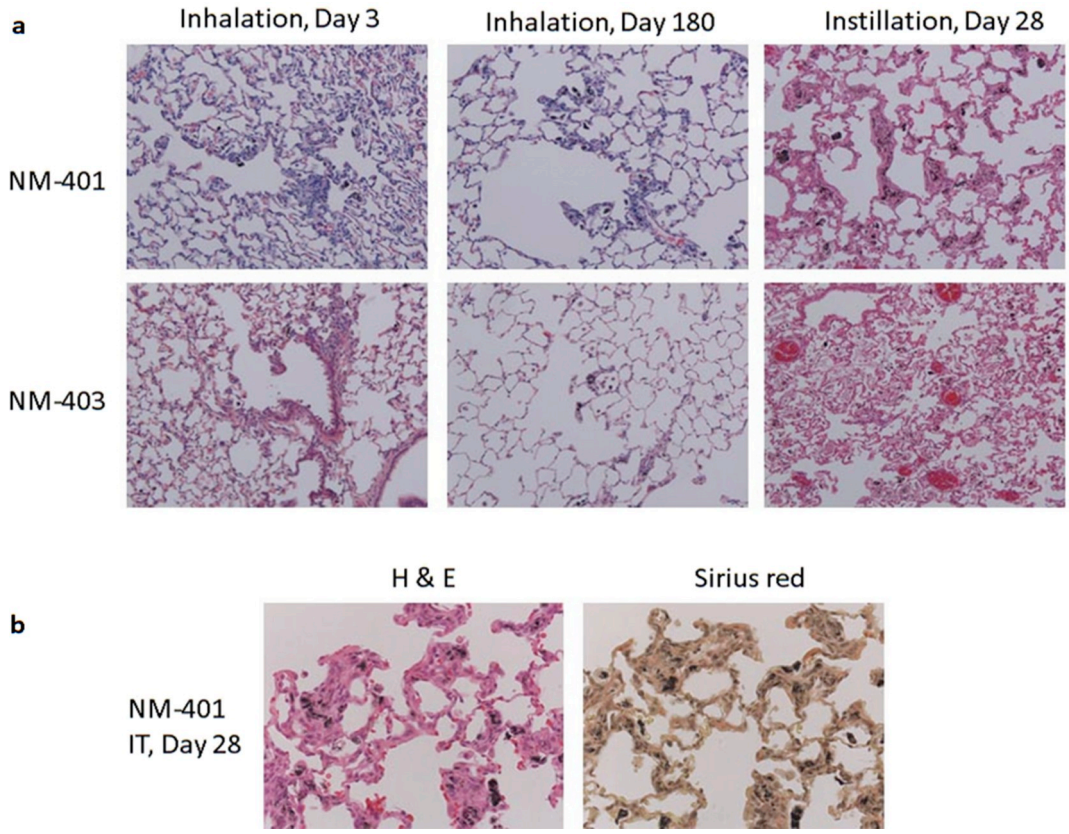

Fig. 8. Histopathological analysis of lung.
(a) Representative photomicrographs of lungs stained with H&E from rats exposed to filtered air or 1.5 mg/m^3 NM-401 or NM-403 aerosols were collected 3 and 180 days after the end of the exposure and a histopathological analysis was performed. Lungs from rats exposed by intratracheal instillation to 540 μg of NM-401 or NM-403 were collected 28 days after exposure. (b) Representative photomicrographs of lungs from animals exposed by intratracheal instillation to NM-401 and stained with H&E or Sirius Red. (For interpretation of the references to colour in this figure legend, the reader is referred to the web version of this article.)

Currently, evidence suggest that MWCNTs with very different physicochemical properties induce very similar toxicological responses in terms of inflammation and acute phase response, whereas only some MWCNTs induce cancer in rodent studies (Muller et al., 2009; Rittinghausen et al., 2014; Poulsen et al., 2015; Kasai et al., 2016). In order to enable design of safer nanomaterials (safer-by-design), we need to be able to compare the toxicity of different nanomaterials, including different MWCNTs, in a cost-effective manner. In this study, we compared the pulmonary toxicity of two well-characterized MWCNTs that were administered by two methods: IT and nose-only inhalation. The main toxicological data of this study are summarized in Table 4. While the latter is considered the gold standard, IT, which is used for hazard assessment, has several disadvantages including skipping of the upper airways and a high dose rate (hundreds of micrograms of MWCNTs are deposited into the lung within seconds by IT while the same amount is deposited for tens or hundreds hours by inhalation) (Oberdorster et al., 2015). The advantage of IT exposure is the better control of the deposited dose, thus allowing comparison of different materials. Some studies comparing the pulmonary toxicity of MWCNTs following IT/pharyngeal aspiration or inhalation have been published (Porter et al., 2010; Morimoto et al., 2012; Porter et al., 2013; Silva et al., 2014). Silva et al. for instance, investigated the effect of pristine and surface modified MWCNTs. While they observed, following IT, a dose dependent increase of inflammation, no such an effect was seen following inhalation because the deposited dose was probably too low (Silva et al., 2014). From these data it was difficult to conclude on the comparability of the two methods to assess the pulmonary toxicity of MWCNTs. Likewise, Morimoto et al. described similar effects with another MWCNT sample (Morimoto et al., 2012). Porter et al., from two independent studies observed that an equivalent deposited dose following inhalation or pharyngeal aspiration in mice induced the same level of granulocytes influx 1 day after the end of exposure (Porter et al., 2010; Porter et al., 2013). However, they did not compare the effect of such exposures at longer post-exposure time points. The experiments described in our study were then designed to try to give additional information regarding the relevance of the two methods of administration for MWCNT hazard assessment across different types of MWCNTs. They focused on the physical and chemical properties of the MWCNTs and their long term pulmonary effects.

In the inhalation studies, MWCNT aerosols were produced with an acoustic generator (McKinney et al., 2009), which gave us the opportunity to produce an aerosol from a nanopowder at very low energy thereby avoiding any alteration of the primary structure of the MWCNTs. Furthermore, acoustic generation is a good surrogate for aerosol production in the occupational setting. The selected aerosol concentrations (0.5 and 1.5 mg/m^3) were based on the work of (MaHock et al., 2009) and (Pauluhn, 2010a), who performed 90-day inhalation toxicity studies with MWCNT materials (Nanocyl NC 7000 and Baytubes, respectively) at 0.1, 0.5 and 2.5 mg/m^3 and 0.1, 0.4, 1.5 and 6 mg/m^3, respectively. In both studies, lung inflammation was detected at 0.4–0.5 mg/m^3. Taking into account the exposure time and assuming equivalent deposited doses, our highest concentration (*i.e.* 1.5 mg/m^3 for 4 weeks) was comparable to exposure to MWCNTs at a concentration of 0.5 mg/m^3 for 90 days. In our experimental set-up, and due to the lower dustiness index of NM-403 (Dazon et al., 2017), 1.5 mg/m^3 was also the highest aerosol concentration of NM-403 for which a stable and reproducible aerosol could be generated.

In contrast, rats were intratracheally instilled at doses of 180 or

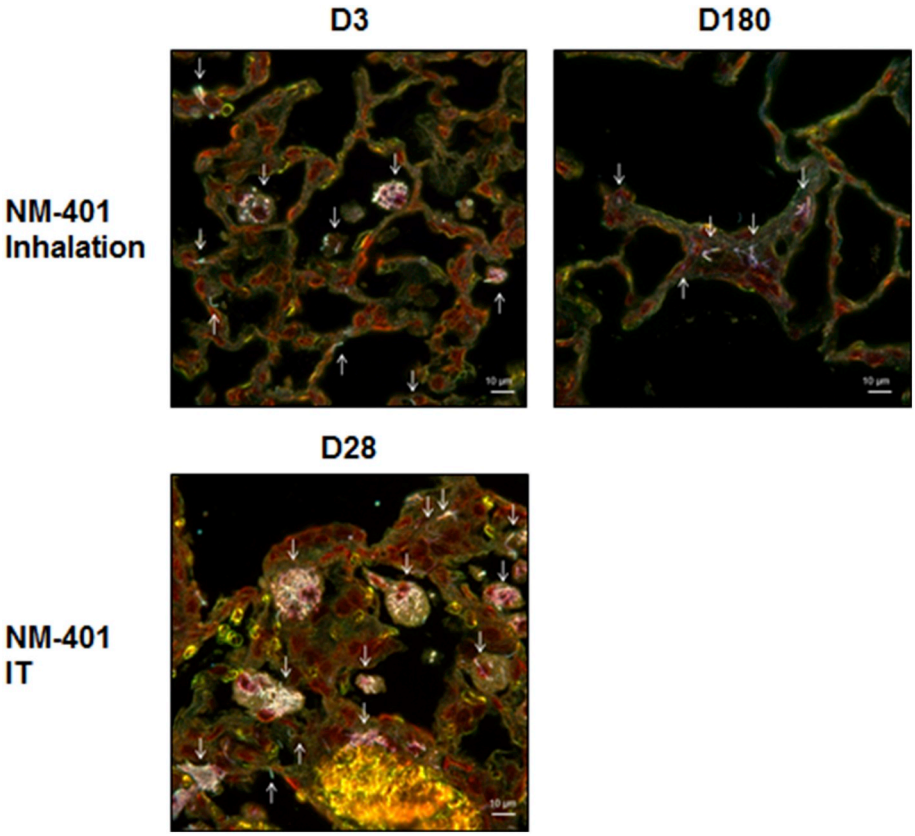

Fig. 9. Enhanced darkfield microscopy analysis of lung.
Pulmonary distribution of MWCNT NM-401 3 days and 180 days after subacute inhalation or 28 days after intratracheal instillation (IT). NM-401 particles (white arrows) are mainly located in alveolar macrophages and are also present as single fibers or bundled fibers at or in alveolar walls. Scale bar 10 µm.

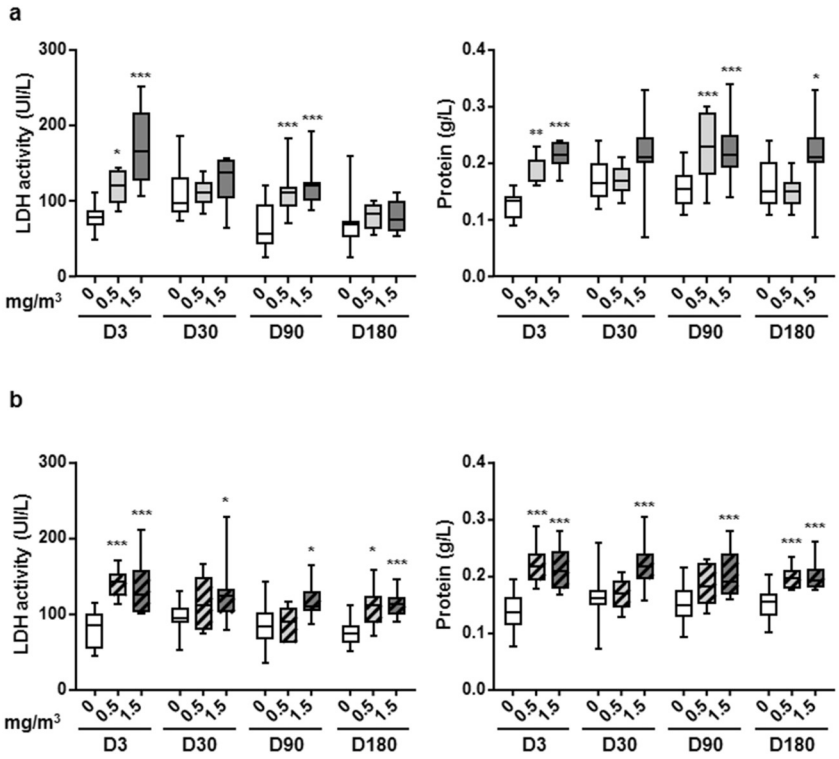

Fig. 10. Study of enzyme activity and protein content in bronchoalveolar lavage fluid.
LDH activity and protein content in BAL fluid were analyzed 3, 30, 90 and 180 days after exposure to filtered air (control animals) or to 0.5 or 1.5 mg/m^3 NM-401 (a) or NM-403 (b) aerosols. * $p < .05$, ** $p < .01$, *** $p < .005$ Significantly different from the control.

540 µg/rat. We have previously shown that MWCNTs are found in all lung lobes following IT exposure (Poulsen et al., 2016).These doses were derived from doses previously administered in mice (18 and 54 µg/mice) (Poulsen et al., 2017), having adjusted the dose to take into account the differences in body weight and ventilation rate in rats and mice. The doses thus correspond to 1 and 3 times the expected 40-year exposure for workers (40 h working week) at the recommended exposure limit of 1 µg MWCNT/m^3 (NIOSH, 2013), when assuming 10% deposition (Ma-Hock et al., 2009), and a ventilation rate of 18 L/h for rat. At the time, no additional interspecies dosimetric adjustment factor

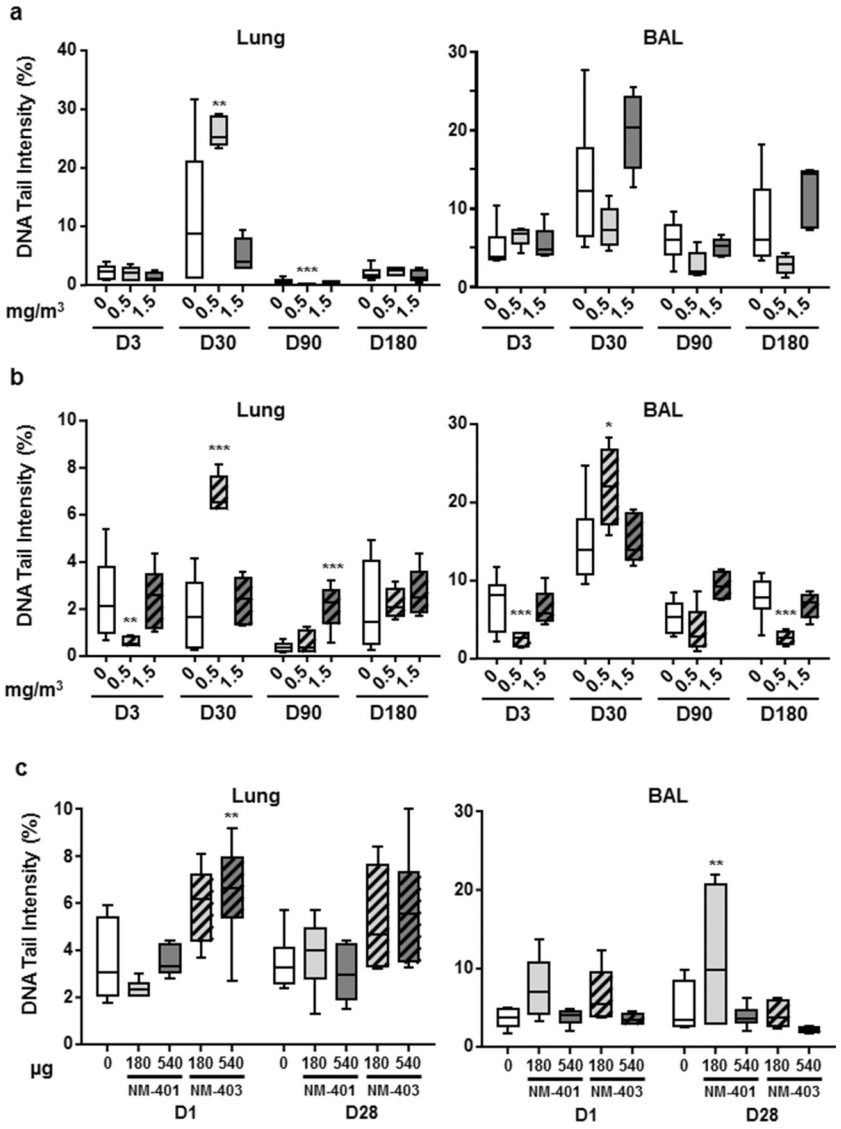

Fig. 11. Effect of NM-401 or NM-403 exposure on DNA damage.
DNA damage was analyzed in lung and BAL fluids by comet assay 3, 30, 90 and 180 days after the inhalation exposure to filtered air (control animals) or to 0.5 or 1.5 mg/m^3 NM-401 (a) or NM-403 (b) aerosols. The comet assay was performed on lung and BAL cells collected 1 and 28 days after intratracheal instillation of 180 or 540 µg of NM-401 or NM-403 (c). * $p < .05$, ** $p < .01$, *** $p < .005$ Significantly different from the control.

was taken into account because, in their calculations, Pauluhn (2010a, b) considered that the increased ventilation of rats is balanced out by the higher respirability of MWCNT particles in humans (Pauluhn, 2010b).

The behavior of the two MWCNTs in the dispersion media and in the aerosol phase was very different: while the "short and thin" NM-403 formed smaller agglomerates than the "long and thick" NM-401 in the dispersion media, it produced larger particles in the aerosol (Fig. 6). This particle size (~2 µm), in addition to its fibrous character (mean aspect ratio = 4), had a direct incidence on the inhalable fraction, which was lower than 40%, and consequently, on the pulmonary deposited amount. Thus, even though the thoracic deposited amounts after inhalation of NM-401 (taking into account the uncertainty related to the estimates from the MPPD model) were similar to (within the same range as) those expected following instillation—706 µg *vs.* 540 µg and 279 µg *vs.* 180 µg, respectively—this was not the case for NM-403 (88 µg *vs.* 540 µg and 22 µg *vs.* 180 µg), which inevitably complicated the comparison of the results. However, these results should be treated with caution since no direct measurement of pulmonary deposited MWCNTs was made. Nevertheless, in the study of Pauluhn (Pauluhn, 2010b), the deposited dose of Baytube, a MWCNT with a shape comparable to that of NM-403, estimated from its cobalt content was about 100 µg/lung following 90-day inhalation of 1.5 mg/m^3 of this MWCNT aerosol. In the current study, the animals were exposed for only one third of this time; the calculated dose deposited in the lung was *ca.* 34 µg/lung, which is in good agreement with Pauluhn's measurements. Considering only the pulmonary deposited fraction of NM-401, the amount deposited after inhalation at the highest concentration is comparable to that deposited by IT at the lowest dose. However, in our study the pulmonary inflammation induced by NM-403 was higher than in the aforementioned study by Pauluhn; while strong inflammation was observed after exposure to 0.5 mg/m^3 of MWCNT for 4 weeks (about 20% of neutrophilic granulocytes out of all BAL cells), a lower inflammatory response was detected in animals exposed to 0.4 mg/m^3 for 90 days (about 10% neutrophilic granulocytes out of all BAL cells). In our inhalation study, the aerosol was generated from an unmodified nanopowder, while in the Pauluhn's study a ball mill was used to micronize the MWCNT agglomerates. This step may have modified the physical properties of the MWCNT, thereby reducing its toxicity. The fact that the rat strains were different (Sprague Dawley *vs.* Wistar rats)

Table 4
Summary of data.

				BAL cytology					BAL biochemistry		Comet assay	
Exposure route	MWCNT	Dose	Time point	Neutro	Lympho	Macro	Eosino	Total cells	LDH activity	Protein	Lung	BAL
Inhalation	NM-401	0.5 mg/m^3	3	–	–	De ***		De **	In *	In **	–	–
			30	–	–	De ***		De ***	–	–	In **	–
			90	–	In ***	–		–	In ***	In ***	De ***	–
			180	–	–	De **		De **	–	–	–	–
		1.5 mg/m^3	3	In ***	In ***	–		In ***	In ***	In ***	–	–
			30	In ***	In ***	–		–	–	–	–	–
			90	In ***	–	De **		–	In ***	In ***	–	–
			180	–	–	De *		–	–	In *	–	–
	NM-403	0.5 mg/m^3	3	In ***	–	–		–	In ***	In ***	De **	De ***
			30	In ***	–	–		–	–	–	In ***	In *
			90	–	–	De ***		De ***	–	–	–	–
			180	In ***	–	–		–	In *	In ***	–	De ***
		1.5 mg/m^3	3	In ***	–	–		–	In ***	In ***	–	–
			30	In ***	–	–		–	In *	In ***	–	–
			90	In ***	–	De *		–	In *	In ***	In ***	–
			180	In ***	–	–		–	In ***	In ***	–	–
Instillation	NM-401	180 µg	1	–	–	–	In ***	–			–	–
			28	–	–	–	–	–			–	In **
		540 µg	1	In *	–	De ***	In ***	In *			–	–
			28	–	In ***	–	–	–			–	–
	NM-403	180 µg	1	In ***	–	De *	In ***	In ***			–	–
			28	–	In *	–	–	–			–	–
		540 µg	1	In ***	–	De **	In ***	In ***			In **	–
			28	In ***	In *	–	–	In ***			–	–

Significantly different from the control. In: increase, De: decrease.
* $p < .05$.
** $p < .01$.
*** $p < .005$.

and that the two MWCNT samples were probably not taken from the same batch might also explain the differences between the two studies.

When the neutrophil influxes from IT and inhalation exposure were plotted against the estimated pulmonary deposited surface area, the data were remarkably well-aligned at two different post-exposure time points (inhalation on day 3/IT on day 1 and inhalation on day 30/IT on day 28, respectively). The observed surface area-dependent inflammatory response at two different time points across instillation and inhalation may suggest that dose rate is of less importance for the inflammatory response to these insoluble fibers.

We have previously shown that the deposited surface area of MWCNTs is a good predictor of pulmonary neutrophil influx, a hallmark of inflammation following mouse exposure (Poulsen et al., 2016), and the present data may suggest that data from sub-acute inhalation studies and IT studies are comparable.

Despite the biopersistence of CNTs in lung tissue and the presence of a pulmonary inflammatory response, no significant histopathological changes were observed following inhalation. In contrast, a fibrotic process was observed following NM-401 administration *via* IT at the highest dose. In NM-403 exposed animals, reactive changes including some alveolar wall thickening were noticed but no definite fibrosis was observed. Interestingly NM-403 exposure also seemed to cause the presence of proteinaceous material in alveoli compatible with pulmonary alveolar proteinosis (PAP). In the literature, differences in outcomes after inhalation and instillation exposure has been explained by the higher deposited dose in the IT study, as fibrosis formation has been shown to be highly dose-dependent (Pauluhn, 2010b). We have previously observed NM-401-induced lung fibrosis in mice, at a higher dose (*ca.* 9 mg/kg) compared to the current study (*ca.* 3 mg/kg) (Poulsen et al., 2015). However no direct measurement of the deposited dose is available.

We found that neutrophil influx correlated well with MWCNT lung deposited surface area. These findings are in good agreement with a previous study that suggested that specific surface area was a good predictor of MWCNT-induced lung inflammation regardless of the length or diameter of the MWCNT (Poulsen et al., 2016). In addition, we observed that following inhalation, the percentage of NM-401 positive alveolar macrophages was twice that of NM-403. This could be in part explained by the number of particles present in the aerosols, which was much lower for NM-403. Moreover, the shape of the MWCNTs found in alveolar macrophages was similar to that observed in the aerosol and collected on a TEM grid, suggesting that the MWCNTs to which the animals were exposed were similar to those found in lungs.

Increased levels of DNA strand breaks were observed across inhalation/instillation, CNT type, doses and time points, but no dose-response relationship and no consistent patterns were observed. Similar lack of dose response relationship has been observed previously for MWCNTs (Poulsen et al., 2015; Poulsen et al., 2016) and for other carbon based nanomaterials (Bourdon et al., 2012; Kyjovska et al., 2015; Bengtson et al., 2017). An absence of significant DNA damage after exposure of rats to MWCNTs by inhalation or IT, as well as in *in vitro* models, has also been reported in other studies (Jackson et al., 2015; Pothmann et al., 2015; Louro et al., 2016; Horibata et al., 2017) In contrast, (Kim et al., 2014) showed a dose-dependent increase in DNA damage at day 90 after exposure of Fischer rats to MWCNTs by inhalation, (Poulsen et al., 2015) showed induction of DNA damage in mouse lung only at day 1 after IT of NM-401, and (Rahman et al., 2017) showed an increase in DNA damage at day 90 after IT of NM-401. Furthermore, Poulsen *et al* showed that DNA strand break levels were predicted by MWCNT diameter, in that increased diameter predicted increased levels of DNA damage. in lung tissue 1 and 28 post-exposure, whereas neither metal content, MWCNT length nor surface hydroxyl levels consistently correlated with genotoxicity (Poulsen et al., 2016). Thus, the study suggested that thick MWCNTs are more genotoxic than thin ones. Several different thick and long MWCNTs have been shown to induce cancer in rats (Rittinghausen et al., 2014; Kasai et al., 2016) whereas one short and thin MWCNT did not induce cancer after IP injection of a relatively high dose (Muller et al., 2009). These data all suggest the importance of CNT physicochemical properties, especially length, diameter and/or specific surface area, for inducing DNA

damage, as well as the importance of the experimental model and post-exposure time used to assess their potential genotoxicity. Moreover, as (Borghini et al., 2017) suggested, for *in vitro* models, increased DNA repair activity could be involved in the absence of observed DNA damage.

It has also been shown that pulmonary exposure to MWCNTs could result in translocation of these particles to other organs (Jacobsen et al., 2017). CNTs have been shown to translocate not only to the lymph nodes (Aiso et al., 2010; Pauluhn, 2010b; Fujita et al., 2016), but also to the pleural cavity, liver, spleen, kidney or bone marrow, brain and uterus, where in certain cases they may exhibit some toxicity (Reddy et al., 2010; Czarny et al., 2014; Xu et al., 2014; Kasai et al., 2016; Knudsen et al., 2019). However, (Shinohara et al., 2016) observed no detectable translocation of CNTs to the liver but did observe long-term retention of CNTs in the lung. Thus, the potential translocation of NM-401 and NM-403 in secondary organs could be useful for understanding the general toxicity of these MWCNTs in animals.

In conclusion, similar dose-response relationship in terms of pulmonary inflammatory response was observed following sub-acute inhalation and a single IT exposure as well as similar genotoxic responses. Even though, the two methods are not totally comparable, this leads us to postulate that IT might be a valuable approach for primary hazard identification and ranking. Since IT allows the deposition of higher doses than inhalation, it seems more sensitive for elucidating the chronic outcomes of animal exposure to MWCNTs. Then, inhalation studies can be reserved to assess the toxicity of nanomaterials of high concern with a more physiological mode of administration taking into account their breathability and other physical and chemical parameters such as dustiness.

Funding information

This work was supported by the European Commission through the EU 7th Framework Programme [Project NanoReg, Grant agreement n° 310584], the EU Horizon 2020 Framework Programme [Project SmartNanoTox, Grant agreement n° 686098] and the Danish Centre for Nanosafety II.

Acknowledgements

The authors gratefully acknowledge Marie-Josèphe Décret, Laurine Douteau and Sylvie Michaux of the INRS laboratory's animal facility for their help in rat handling and husbandry, Anne-Marie Lambert-Xolin for the biochemistry analyses, and Cristina Langlais, Yves Guichard and Caroline Fontana for their technical help in the comet assay.

Conflict of interest

The authors declare that they have no competing interests.

References

Aiso, S., Yamazaki, K., Umeda, Y., Asakura, M., Kasai, T., Takaya, M., Toya, T., Koda, S., Nagano, K., Arito, H., Fukushima, S., 2010. Pulmonary toxicity of intratracheally instilled multiwall carbon nanotubes in male Fischer 344 rats. Ind. Health 48, 783–795.

Anjilvel, S., Asgharian, B., 1995. A multiple-path model of particle deposition in the rat lung. Fundam. Appl. Toxicol. 28, 41–50.

Bengtson, S., Knudsen, K.B., Kyjovska, Z.O., Berthing, T., Skaug, V., Levin, M., Koponen, I.K., Shivayogimath, A., Booth, T.J., Alonso, B., Pesquera, A., Zurutuza, A., Thomsen, B.L., Troelsen, J.T., Jacobsen, N.R., Vogel, U., 2017. Differences in inflammation and acute phase response but similar genotoxicity in mice following pulmonary exposure to graphene oxide and reduced graphene oxide. PLoS One 12, e0178355.

Borghini, A., Roursgaard, M., Andreassi, M.G., Kermanizadeh, A., Moller, P., 2017. Repair activity of oxidatively damaged DNA and telomere length in human lung epithelial cells after exposure to multi-walled carbon nanotubes. Mutagenesis 32, 173–180.

Bourdon, J.A., Saber, A.T., Jacobsen, N.R., Jensen, K.A., Madsen, A.M., Lamson, J.S., Wallin, H., Moller, P., Loft, S., Yauk, C.L., Vogel, U.B., 2012. Carbon black nanoparticle instillation induces sustained inflammation and genotoxicity in mouse lung and liver. Part Fibre Toxicol 9, 5.

Cosnier, F., Bau, S., Grossmann, S., Nunge, H., Brochard, C., Viton, S., Payet, R., Witschger, O., Gate, L., 2016. Design and characterization of an inhalation system to expose rodents to Nanoaerosols. Aerosol Air Qual. Res. 16, 2989–3000.

Czarny, B., Georgin, D., Berthon, F., Plastow, G., Pinault, M., Patriarche, G., Thuleau, A., L'Hermite, M.M., Taran, F., Dive, V., 2014. Carbon nanotube translocation to distant organs after pulmonary exposure: insights from in situ (14)C-radiolabeling and tissue radioimaging. ACS Nano 8, 5715–5724.

Dazon, C., Witschger, O., Bau, S., Payet, R., Beugnon, K., Petit, G., Garin, T., Martinon, L., 2017. Dustiness of 14 carbon nanotubes using the vortex shaker method. In: 5th Nanosafe International Conference on Health and Safety Issues Related to Nanomaterials for a Socially Responsible Approach. 7–10 November 2016 – MINATEC, Grenoble. France.

Donaldson, K., Oberdorster, G., 2011. Continued controversy on chrysotile biopersistence. Int. J. Occup. Environ. Health 17, 98–102.

Donaldson, K., Poland, C.A., Murphy, F.A., MacFarlane, M., Chernova, T., Schinwald, A., 2013. Pulmonary toxicity of carbon nanotubes and asbestos – similarities and differences. Adv. Drug Deliv. Rev. 65, 2078–2086.

Doudrick, K., Corson, N., Oberdorster, G., Eder, A.C., Herckes, P., Halden, R.U., Westerhoff, P., 2013. Extraction and quantification of carbon nanotubes in biological matrices with application to rat lung tissue. ACS Nano 7, 8849–8856.

Fujita, K., Fukuda, M., Endoh, S., Maru, J., Kato, H., Nakamura, A., Shinohara, N., Uchino, K., Honda, K., 2016. Pulmonary and pleural inflammation after intratracheal instillation of short single-walled and multi-walled carbon nanotubes. Toxicol. Lett. 257, 23–37.

Guichard, Y., Maire, M.A., Sebillaud, S., Fontana, C., Langlais, C., Micillino, J.C., Darne, C., Roszak, J., Stepnik, M., Fessard, V., Binet, S., Gate, L., 2015. Genotoxicity of synthetic amorphous silica nanoparticles in rats following short-term exposure. Part 2: intratracheal instillation and intravenous injection. Environ. Mol. Mutagen. 56, 228–244.

Hamilton Jr., R.F., Wu, Z., Mitra, S., Shaw, P.K., Holian, A., 2013. Effect of MWCNT size, carboxylation, and purification on in vitro and in vivo toxicity, inflammation and lung pathology. Part Fibre Toxicol 10, 57.

Horibata, K., Ukai, A., Ogata, A., Nakae, D., Ando, H., Kubo, Y., Nagasawa, A., Yuzawa, K., Honma, M., 2017. Absence of in vivo mutagenicity of multi-walled carbon nanotubes in single intratracheal instillation study using F344 gpt delta rats. Genes Environ 39, 4.

IARC, 2017. Some Nanomaterials and Some Fibres. IARC Monographs on the Evaluation of Carcinogenic Risks to Humans. vol. 111. pp. 35–214.

Jackson, P., Vogel, U., Wallin, H., Hougaard, K.S., 2011. Prenatal exposure to carbon black (printex 90): effects on sexual development and neurofunction. Basic Clin. Pharmacol. Toxicol 109, 434–437.

Jackson, P., Pedersen, L.M., Kyjovska, Z.O., Jacobsen, N.R., Saber, A.T., Hougaard, K.S., Vogel, U., Wallin, H., 2013. Validation of freezing tissues and cells for analysis of DNA strand break levels by comet assay. Mutagenesis 28, 699–707.

Jackson, P., Kling, K., Jensen, K.A., Clausen, P.A., Madsen, A.M., Wallin, H., Vogel, U., 2015. Characterization of genotoxic response to 15 multiwalled carbon nanotubes with variable physicochemical properties including surface functionalizations in the FE1-Muta(TM) mouse lung epithelial cell line. Environ. Mol. Mutagen. 56, 183–203.

Jacobsen, N.R., Stoeger, T., van den Brule, S., Saber, A.T., Beyerle, A., Vietti, G., Mortensen, A., Szarek, J., Budtz, H.C., Kermanizadeh, A., Banerjee, A., Ercal, N., Vogel, U., Wallin, H., Moller, P., 2015. Acute and subacute pulmonary toxicity and mortality in mice after intratracheal instillation of ZnO nanoparticles in three laboratories. Food Chem. Toxicol. 85, 84–95.

Jacobsen, N.R., Moller, P., Clausen, P.A., Saber, A.T., Micheletti, C., Jensen, K.A., Wallin, H., Vogel, U., 2017. Biodistribution of carbon nanotubes in animal models. Basic Clin. Pharmacol. Toxicol 121 (Suppl. 3), 30–43.

Rasmussen, K., Mast, J., De Temmerman, P.J., Verleysen, E., Waegeneers, N., Van Steen, F., Pizzolon, J.C., De Temmerman, L., Van Doren, E., Jensen, K.A., Birkedal, R., Clausen, P.A., Kembouche, Y., Thieriet, N., Spalla, O., Giuot, C., Rousset, D., Witschger, O., Bau, S., Bianchi, B., Shivachev, B., Dimowa, L., Nikolova, R., Nihtianova, D., Tarassov, M., Petrov, O., Bakardjieva, S., Motzkus, C., Labarraque, G., Oster, C., Cotogno, G., Gaillard, C., 2014. Multi-walled carbon nanotubes, NM-400, NM-401, NM-402, NM-403: Characterisation and physico-chemical properties. JRC repository : NM-series of representative manufactured nanomaterials. Publications Office of the European Union, pp. 118. Available at. http://publications.jrc.ec.europa.eu/repository/handle/JRC91205.

Kasai, T., Umeda, Y., Ohnishi, M., Kondo, H., Takeuchi, T., Aiso, S., Nishizawa, T., Matsumoto, M., Fukushima, S., 2015. Thirteen-week study of toxicity of fiber-like multi-walled carbon nanotubes with whole-body inhalation exposure in rats. Nanotoxicology 9, 413–422.

Kasai, T., Umeda, Y., Ohnishi, M., Mine, T., Kondo, H., Takeuchi, T., Matsumoto, M., Fukushima, S., 2016. Lung carcinogenicity of inhaled multi-walled carbon nanotube in rats. Part Fibre Toxicol 13, 53.

Kim, J.S., Sung, J.H., Choi, B.G., Ryu, H.Y., Song, K.S., Shin, J.H., Lee, J.S., Hwang, J.H., Lee, J.H., Lee, G.H., Jeon, K., Ahn, K.H., Yu, I.J., 2014. In vivo genotoxicity evaluation of lung cells from Fischer 344 rats following 28 days of inhalation exposure to MWCNTs, plus 28 days and 90 days post-exposure. Inhal. Toxicol. 26, 222–234.

Knudsen, K.B., Berthing, T., Jackson, P., Poulsen, S.S., Mortensen, A., Jacobsen, N.R., Skaug, V., Szarek, J., Hougaard, K.S., Wolff, H., Wallin, H., Vogel, U., 2019. Physicochemical predictors of multi-walled carbon nanotube-induced pulmonary histopathology and toxicity one year after pulmonary deposition of 11 different multi-walled carbon nanotubes in mice. Basic Clin. Pharmacol. Toxicol 124, 211–227.

Kyjovska, Z.O., Jacobsen, N.R., Saber, A.T., Bengtson, S., Jackson, P., Wallin, H., Vogel, U., 2015. DNA damage following pulmonary exposure by instillation to low doses of carbon black (Printex 90) nanoparticles in mice. Environ. Mol. Mutagen. 56, 41–49.

Louro, H., Pinhao, M., Santos, J., Tavares, A., Vital, N., Silva, M.J., 2016. Evaluation of the cytotoxic and genotoxic effects of benchmark multi-walled carbon nanotubes in relation to their physicochemical properties. Toxicol. Lett. 262, 123–134.
Ma-Hock, L., Treumann, S., Strauss, V., Brill, S., Luizi, F., Mertler, M., Wiench, K., Gamer, A.O., van Ravenzwaay, B., Landsiedel, R., 2009. Inhalation toxicity of multiwall carbon nanotubes in rats exposed for 3 months. Toxicol. Sci. 112, 468–481.
McKinney, W., Chen, B., Frazer, D., 2009. Computer controlled multi-walled carbon nanotube inhalation exposure system. Inhal. Toxicol. 21, 1053–1061.
Miller, F.J., Asgharian, B., Schroeter, J.D., Price, O., Corley, R.A., Einstein, D.R., Jacob, R.E., Cox, T.C., Kabilan, S., Bentley, T., 2014. Respiratory tract lung geometry and dosimetry model for male Sprague-Dawley rats. Inhal. Toxicol. 26, 524–544.
Miller, F.J., Asgharian, B., Schroeter, J.D., Price, O., 2016. Improvements and additions to the multiple path particle dosimetry model. J. Aerosol Sci. 99, 14–26.
Morimoto, Y., Hirohashi, M., Ogami, A., Oyabu, T., Myojo, T., Todoroki, M., Yamamoto, M., Hashiba, M., Mizuguchi, Y., Lee, B.W., Kuroda, E., Shimada, M., Wang, W.N., Yamamoto, K., Fujita, K., Endoh, S., Uchida, K., Kobayashi, N., Mizuno, K., Inada, M., Tao, H., Nakazato, T., Nakanishi, J., Tanaka, I., 2012. Pulmonary toxicity of well-dispersed multi-wall carbon nanotubes following inhalation and intratracheal instillation. Nanotoxicology 6, 587–599.
Muller, J., Delos, M., Panin, N., Rabolli, V., Huaux, F., Lison, D., 2009. Absence of carcinogenic response to multiwall carbon nanotubes in a 2-year bioassay in the peritoneal cavity of the rat. Toxicol. Sci. 110, 442–448.
NIOSH, 2013. Occupational exposure to carbon nantubes and nanofibers. Curr. Intell. Bull 65.
Oberdorster, G., Castranova, V., Asgharian, B., Sayre, P., 2015. Inhalation exposure to carbon nanotubes (CNT) and carbon nanofibers (CNF): methodology and dosimetry. J. Toxicol. Environ. Health B Crit. Rev 18, 121–212.
Ohnishi, M., Suzuki, M., Yamamoto, M., Kasai, T., Kano, H., Senoh, H., Higashikubo, I., Araki, A., Fukushima, S., 2016. Improved method for measurement of multi-walled carbon nanotubes in rat lung. J. Occup. Med. Toxicol 11.
Pauluhn, J., 2010a. Multi-walled carbon nanotubes (Baytubes): approach for derivation of occupational exposure limit. Regul. Toxicol. Pharmacol. 57, 78–89.
Pauluhn, J., 2010b. Subchronic 13-week inhalation exposure of rats to multiwalled carbon nanotubes: toxic effects are determined by density of agglomerate structures, not fibrillar structures. Toxicol. Sci. 113, 226–242.
Pauluhn, J., Rosenbruch, M., 2015. Lung burdens and kinetics of multi-walled carbon nanotubes (Baytubes) are highly dependent on the disaggregation of aerosolized MWCNT. Nanotoxicology 9, 242–252.
Porter, D.W., Hubbs, A.F., Mercer, R.R., Wu, N., Wolfarth, M.G., Sriram, K., Leonard, S., Battelli, L., Schwegler-Berry, D., Friend, S., Andrew, M., Chen, B.T., Tsuruoka, S., Endo, M., Castranova, V., 2010. Mouse pulmonary dose- and time course-responses induced by exposure to multi-walled carbon nanotubes. Toxicology 269, 136–147.
Porter, D.W., Hubbs, A.F., Chen, B.T., McKinney, W., Mercer, R.R., Wolfarth, M.G., Battelli, L., Wu, N., Sriram, K., Leonard, S., Andrew, M., Willard, P., Tsuruoka, S., Endo, M., Tsukada, T., Munekane, F., Frazer, D.G., Castranova, V., 2013. Acute pulmonary dose-responses to inhaled multi-walled carbon nanotubes. Nanotoxicology 7, 1179–1194.
Pothmann, D., Simar, S., Schuler, D., Dony, E., Gaering, S., Le Net, J.L., Okazaki, Y., Chabagno, J.M., Bessibes, C., Beausoleil, J., Nesslany, F., Regnier, J.F., 2015. Lung inflammation and lack of genotoxicity in the comet and micronucleus assays of industrial multiwalled carbon nanotubes Graphistrength((c)) C100 after a 90-day nose-only inhalation exposure of rats. Part Fibre Toxicol 12, 21.
Poulsen, S.S., Saber, A.T., Williams, A., Andersen, O., Kobler, C., Atluri, R., Pozzebon, M.E., Mucelli, S.P., Simion, M., Rickerby, D., Mortensen, A., Jackson, P., Kyjovska, Z.O., Molhave, K., Jacobsen, N.R., Jensen, K.A., Yauk, C.L., Wallin, H., Halappanavar, S., Vogel, U., 2015. MWCNTs of different physicochemical properties cause similar inflammatory responses, but differences in transcriptional and histological markers of fibrosis in mouse lungs. Toxicol. Appl. Pharmacol. 284, 16–32.
Poulsen, S.S., Jackson, P., Kling, K., Knudsen, K.B., Skaug, V., Kyjovska, Z.O., Thomsen, B.L., Clausen, P.A., Atluri, R., Berthing, T., Bengtson, S., Wolff, H., Jensen, K.A., Wallin, H., Vogel, U., 2016. Multi-walled carbon nanotube physicochemical properties predict pulmonary inflammation and genotoxicity. Nanotoxicology 10, 1263–1275.
Poulsen, S.S., Knudsen, K.B., Jackson, P., Weydahl, I.E., Saber, A.T., Wallin, H., Vogel, U., 2017. Multi-walled carbon nanotube-physicochemical properties predict the systemic acute phase response following pulmonary exposure in mice. PLoS One 12, e0174167.
Rahman, L., Jacobsen, N.R., Aziz, S.A., Wu, D., Williams, A., Yauk, C.L., White, P., Wallin, H., Vogel, U., Halappanavar, S., 2017. Multi-walled carbon nanotube-induced genotoxic, inflammatory and pro-fibrotic responses in mice: investigating the mechanisms of pulmonary carcinogenesis. Mutat. Res. 823, 28–44.
Ravichandran, P., Baluchamy, S., Gopikrishnan, R., Biradar, S., Ramesh, V., Goornavar, V., Thomas, R., Wilson, B.L., Jeffers, R., Hall, J.C., Ramesh, G.T., 2011. Pulmonary biocompatibility assessment of inhaled single-wall and multiwall carbon nanotubes in BALB/c mice. J. Biol. Chem. 286, 29725–29733.
Reddy, A.R., Krishna, D.R., Reddy, Y.N., Himabindu, V., 2010. Translocation and extra pulmonary toxicities of multi wall carbon nanotubes in rats. Toxicol. Mech. Methods 20, 267–272.
Rittinghausen, S., Hackbarth, A., Creutzenberg, O., Ernst, H., Heinrich, U., Leonhardt, A., Schaudien, D., 2014. The carcinogenic effect of various multi-walled carbon nanotubes (MWCNTs) after intraperitoneal injection in rats. Part Fibre Toxicol 11, 59.
Shinohara, N., Nakazato, T., Ohkawa, K., Tamura, M., Kobayashi, N., Morimoto, Y., Oyabu, T., Myojo, T., Shimada, M., Yamamoto, K., Tao, H., Ema, M., Naya, M., Nakanishi, J., 2016. Long-term retention of pristine multi-walled carbon nanotubes in rat lungs after intratracheal instillation. J. Appl. Toxicol. 36, 501–509.
Silva, R.M., Doudrick, K., Franzi, L.M., TeeSy, C., Anderson, D.S., Wu, Z., Mitra, S., Vu, V., Dutrow, G., Evans, J.E., Westerhoff, P., Van Winkle, L.S., Raabe, O.G., Pinkerton, K.E., 2014. Instillation versus inhalation of multiwalled carbon nanotubes: exposure-related health effects, clearance, and the role of particle characteristics. ACS Nano 8, 8911–8931.
Statistica, 2019. https://www.statista.com/statistics/714708/carbon-nanotube-global-market-size-by-application/.
Suzui, M., Futakuchi, M., Fukamachi, K., Numano, T., Abdelgied, M., Takahashi, S., Ohnishi, M., Omori, T., Tsuruoka, S., Hirose, A., Kanno, J., Sakamoto, Y., Alexander, D.B., Alexander, W.T., Jiegou, X., Tsuda, H., 2016. Multiwalled carbon nanotubes intratracheally instilled into the rat lung induce development of pleural malignant mesothelioma and lung tumors. Cancer Sci. 107, 924–935.
Taylor, A.J., McClure, C.D., Shipkowski, K.A., Thompson, E.A., Hussain, S., Garantziotis, S., Parsons, G.N., Bonner, J.C., 2014. Atomic layer deposition coating of carbon nanotubes with aluminum oxide alters pro-fibrogenic cytokine expression by human mononuclear phagocytes in vitro and reduces lung fibrosis in mice in vivo. PLoS One 9, e106870.
van Berlo, D., Wilhelmi, V., Boots, A.W., Hullmann, M., Kuhlbusch, T.A., Bast, A., Schins, R.P., Albrecht, C., 2014. Apoptotic, inflammatory, and fibrogenic effects of two different types of multi-walled carbon nanotubes in mouse lung. Arch. Toxicol. 88, 1725–1737.
Wang, X., Katwa, P., Podila, R., Chen, P., Ke, P.C., Rao, A.M., Walters, D.M., Wingard, C.J., Brown, J.M., 2011. Multi-walled carbon nanotube instillation impairs pulmonary function in C57BL/6 mice. Part Fibre Toxicol 8, 24.
Wang, J., Bahk, Y.K., Chen, S.C., Pui, D.Y.H., 2015. Characteristics of airborne fractal-like agglomerates of carbon nanotubes. Carbon 93, 441–450.
Xu, J., Alexander, D.B., Futakuchi, M., Numano, T., Fukamachi, K., Suzui, M., Omori, T., Kanno, J., Hirose, A., Tsuda, H., 2014. Size- and shape-dependent pleural translocation, deposition, fibrogenesis, and mesothelial proliferation by multiwalled carbon nanotubes. Cancer Sci. 105, 763–769.
Yamashita, K., Yoshioka, Y., Higashisaka, K., Morishita, Y., Yoshida, T., Fujimura, M., Kayamuro, H., Nabeshi, H., Yamashita, T., Nagano, K., Abe, Y., Kamada, H., Kawai, Y., Mayumi, T., Yoshikawa, T., Itoh, N., Tsunoda, S., Tsutsumi, Y., 2010. Carbon nanotubes elicit DNA damage and inflammatory response relative to their size and shape. Inflammation 33, 276–280.